

Generalized characteristic model for lithography: application to negative chemically amplified resists

David H. Ziger*
Chris A. Mack
Romelia Distasio
SEMATECH
2706 Montopolis Drive
Austin, Texas 78741

Abstract. A generalized approach to modeling resist performance is introduced and applied toward characterizing a negative chemically amplified resist system. The Generalized Characteristic Model for lithography is used to extract parameters to evaluate easily development rates from characteristic curves. The model suggests that two lumped parameters, αn and E_0 , dominate lithographic response for negative chemically amplified resists. Both αn and E_0 were regressed from characteristic curves over a postexposure bake temperature and time range from 110 to 150°C and 30 to 90 s and develop times from 30 to 150 s. The parameter E_0 showed the predicted postexposure bake temperature and time and develop time dependencies over the processing window, while αn did not. Possible explanations for this discrepancy are discussed. These parameters were used to simulate linewidths that were compared with experimental results. Linewidth predictions using parameters extracted with the generalized characteristic model agreed to within 15% of experimental results over the entire processing window.

Subject terms: lithography; modeling, negative chemically amplified resists. Optical Engineering 31(1), 98-104 (January 1992).

1 Introduction

Chemically amplified positive and negative resists have demonstrated subhalf-micron resolution and the high sensitivity required for DUV and e-beam lithographies.^{1,2} Current modeling of these systems postulates acid-catalyzed crosslinking of polyvinylphenol (PVP) or deblocking of PVP derivatives for the dissolution inhibition mechanism for negative and positive versions, respectively.^{1,3-5} Consequently, the proposed kinetic mechanisms are quite different though their performance in terms of sensitivity and resolution is similar.

Negative chemically amplified resist systems have been modeled most frequently. Thackeray et al.¹ proposed a mechanism for Shipley SNR248, which is an acid-catalyzed negative resist whose base resin, PVP, is base soluble. Irradiation decomposes a photoacid generator (PAG), which in turn catalyzes the reaction of a melamine crosslinking agent with the PVP resin, thus making it insoluble. Seligson and coworkers^{3,4} developed the concept of "effective dose" to correlate the effect of crosslinking bake kinetics on actual exposure dose. Fukuda and Okazaki⁶ evaluated kinetic parameters for crosslinking and simulated linewidths. Ferguson et al.⁷ and Chiu et al.⁸ have developed a generalized program to extract kinetic parameters from dissolution rate monitoring (DRM) data given proposed reactions.

In this paper, we apply the Generalized Characteristic Model (GCM) to negative chemically amplified resists.⁹ In this general approach, the dissolution mechanism is assumed to be primarily influenced by the solubility of a dominant

soluble species. For SNR248 and similar negative resists, this dominant soluble species is the concentration of unreacted PVP sites. We derive an expression for the unreacted soluble site concentration and the rate of dissolution as a function of dose deposited in the film. Under conditions of minimal bleaching, absorption, and surface dissolution effects, we can extract kinetic parameters from conventional characteristic exposure curves, which relate remaining resist thickness after development as a function of exposure dose.

Characteristic curves were carefully measured over a wide range of experimental conditions. Relevant parameters were then extracted from experimental characteristic curves for SNR248 and compared to model predictions. Finally, simulations were performed using the regressed parameters and compared to experimental results over a wide range of conditions for SNR248.

2 Theory

A detailed explanation of the GCM for lithography is given elsewhere.⁹ The objective of this approach is to extract relevant processing parameters from easily measured lithographic characteristic curves. These parameters are then used in simulation programs. We outline the approach specifically applied toward modeling negative chemically amplified resists.

The characteristic curve quantifies resist remaining after development as a function of incident exposure energy. For current practices of microlithography, resist loss can occur due to the postexposure bake (PEB) shrinkage, $\Delta\tau_{\text{PEB}}$, and dissolution during development, $\Delta\tau_{\text{DEV}}$:

$$\tau_N = 1 - \Delta\tau_{\text{PEB}} - \Delta\tau_{\text{DEV}}, \quad (1)$$

where τ_N is the remaining resist after development nor-

*Current address: AT&T Bell Laboratories, 555 Union Boulevard, Allentown, Pennsylvania 18103.

malized to the initial film thickness. Thus, $\tau_{N(E)}$ is the characteristic curve.

The resist is modeled as a mixture of base soluble, $[S]$, and insoluble, $[M]$, species. Both $\Delta\tau_{PEB}$ and $\Delta\tau_{DEV}$ are dependent on the relative concentrations of these species. For negative chemically amplified resists $[S]$ is the concentration of unreacted host polymer (e.g., PVP). Since the effect of the postexposure bake is to insolubilize the exposed regions via reaction of the host polymer matrix, $\Delta\tau_{PEB}$ is assumed to be linearly dependent on the extent of conversion of $[S]$ to $[M]$:

$$\Delta\tau_{PEB} = \Delta\tau_{(E=0)} + \left(1 - \frac{[S]}{[S_0]}\right)G, \quad (2)$$

where $\Delta\tau_{(E=0)}$ is the normalized thickness change due to the postexposure bake in the unexposed resist, G is the fractional thickness change less $\Delta\tau_{(E=0)}$ at complete conversion, and $[S_0]$ is the initial concentration of soluble sites. (Note that G is a function of initial resist composition.)

Thickness loss during development, $\Delta\tau_{DEV}$, is obtained by integrating the development rate over the time of develop:

$$\Delta\tau_{DEV} = \frac{\int_0^{t_{DEV}} r_{DEV} dt}{D}, \quad (3)$$

where r_{DEV} is the instantaneous develop rate. If absorption, bleaching, reflections, and surface dissolution effects are minimal, then r_{DEV} can be assumed constant yielding:

$$\Delta\tau_{DEV} = \frac{r_{DEV}t_{DEV}}{D}. \quad (4)$$

We assume that the development rate is proportional to the concentration of soluble sites raised to a power n , where n is a coordination number for the number of soluble sites that act in concert to influence solubility*:

$$\Delta\tau_{DEV} = \frac{k_{DEV}t_{DEV}[S]^n}{D}. \quad (5)$$

The concentration of soluble sites $[S]$ for chemically amplified negative resists is obtained from the extent of reaction of the acid-catalyzed postexposure bake chemistry:

$$\frac{d[S]}{dt_{PEB}} = -k_{PEB}[S][H^+], \quad (6)$$

where t_{PEB} and k_{PEB} are the postexposure bake time and rate constant, respectively, and $[H^+]$ is the acid concentration. If acid loss via side reaction (i.e., termination) and diffusion are minimal, then $[H^+]$ can be assumed to remain constant during the postexposure bake. Integrating this pseudo first-order reaction yields:

$$[S] = [S_0] \exp(-k_{PEB}[H^+]t_{PEB}) \quad (7)$$

The PAG decomposes on radiation of energy E to form protons ($\text{PAG} \xrightarrow{h\nu} H^+$). Assuming first-order decomposition photochemistry:

$$\frac{d[\text{PAG}]}{dE} = -k_{\text{photo}}[\text{PAG}], \quad (8)$$

where k_{photo} is the exposure rate constant. Integrating yields:

$$[\text{PAG}] = [\text{PAG}_0] \exp(-k_{\text{photo}}E), \quad (9)$$

where $[\text{PAG}_0]$ is the initial PAG concentration. Acid catalysis is sensitive to residual amine contaminants. For a given amine concentration in the photoresist, an equal amount of acid will be consumed in a neutralization reaction. Thus, the actual acid concentration will be $[H^+] = [\text{PAG}_0] - [\text{PAG}] - [\text{amines}]$. We can relate $[\text{amines}]$ to an effective inhibition dose, E_{inhib} , which is required to generate enough acid to neutralize the amines. From Eq. (9), $[\text{amines}] = [\text{PAG}_0][1 - \exp(-k_{\text{photo}}E_{\text{inhib}})]$. Thus the acid concentration that is available to catalyze the base insolubilizing reaction will be:

$$[H^+] = [\text{PAG}_0] \mathcal{A} \exp(-k_{\text{photo}}E_{\text{inhib}}) \quad (10)$$

where $\mathcal{A} = 1 - \exp[-k_{\text{photo}}(E - E_{\text{inhib}})]$. Substituting Eq. (10) into Eq. (7) yields the concentration of $[S]$:

$$[S] = [S_0] \exp[-\alpha \mathcal{A} \exp(-k_{\text{photo}}E_{\text{inhib}})], \quad (11)$$

where $\alpha = [\text{PAG}_0]k_{PEB}t_{PEB}$. Combining Eqs. (11) and (5) and the result into Eq. (1) provides an expression for τ_N :

$$\tau_N = 1 - \Delta\tau_{PEB} - \mathcal{H} \exp[-\alpha n \mathcal{A} \exp(-k_{\text{photo}}E_{\text{inhib}})], \quad (12)$$

where

$$\mathcal{H} = \frac{k_{DEV}t_{DEV}[S_0]^n}{D}$$

$$\Delta\tau_{PEB} = \Delta\tau_{(E=0)} + G\{1 - \exp[-\alpha \mathcal{A} \exp(-k_{\text{photo}}E_{\text{inhib}})]\}.$$

By definition, $E = E_0$ when $\tau_N = 0$. (E_0 is commonly referred to as the gel dose for negative resists.) Consequently, we can solve Eq. (12) for $(k_{DEV}t_{DEV}[S_0]^n)/D$ in terms of E_0 , which simplifies to:

$$\tau_N = 1 - \Delta\tau_{PEB} - (1 - \Delta\tau_{PEB,E_0}) \cdot \exp\{-\alpha n[\exp(-k_{\text{photo}}E_0) - \exp(-k_{\text{photo}}E)]\}, \quad (13)$$

where $\Delta\tau_{PEB,E_0}$ is the thickness loss due to PEB at E_0 . Note that with algebraic simplification, E_{inhib} is not an independent parameter but is lumped into E_0 (see Sec. 5.3). The developing rate r_{DEV} is

$$r_{DEV} = \frac{D}{t_{DEV}}(1 - \Delta\tau_{PEB,E_0}) \cdot \exp\{-\alpha n[\exp(-k_{\text{photo}}E_0) - \exp(-k_{\text{photo}}E)]\} \quad (14)$$

Therefore, if αn and E_0 can be extracted from τ_N , r_{DEV} can be easily evaluated. This rate expression can then be used in conjunction with lithography simulation programs to predict linewidths.

*See Sec. 4.2 for comparisons of this develop model to other approaches. Mack¹⁰ and Trefonas and Daniels¹¹ have arrived at similar equations for modeling DRM data for positive photoresists.

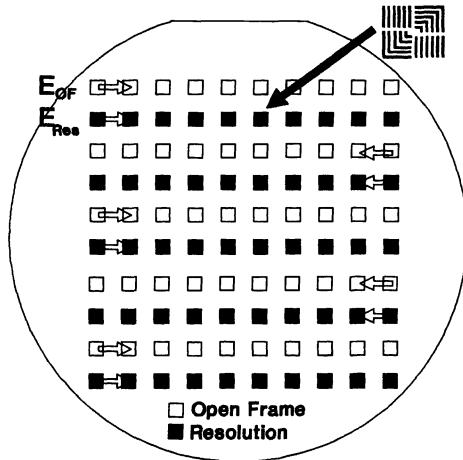


Fig. 1 Two-pass exposure pattern.

3 Experimental

The objective of the experimental work was to extract relevant parameters, αn and E_0 , from measured characteristic curves under various postexposure bake and develop conditions. These parameters were used to evaluate r_{DEV} . The lithographic simulation program PROLITH/2 used αn and E_0 to simulate linewidths, which were then compared to experimental results.⁹

Silicon wafers coated with SNR248 resist on a DUV-3 antireflection coating were exposed on a 0.35-NA Laserstep KrF stepper. The actinic wavelength was 248 nm. An antireflection coating was used to minimize substrate reflections. Postexposure bake was done using Flexifab tracks followed by batch develop in 0.135 normal TMAH. Figure 1 shows the two-pass exposure pattern that was used. The first pass was a serpentine of increasing open frame exposures, while the second pass interwound a serpentine of resolution die of increasing doses. Resist thickness measurements were taken at the open frame exposure sites. An SM200/E Spectramap was used to measure resist thickness after softbake and postexposure bake while an FT500 Spectramap was used to measure final resist thickness after development. Using this technique $\Delta\tau_{DEV}$, and in principle $\Delta\tau_{PEB}$, could be measured.

Wafers with the pattern in Fig. 1 were processed at five postexposure bake temperatures and times and develop times. Ranges of experimental T_{PEB} , t_{PEB} , and t_{DEV} conditions are shown in Table 1. These wafers were processed randomly in the same day. This was done to minimize systematic error when comparing model predictions with experimental measurements of αn and E_0 . Furthermore, the centerpoint conditions, $T_{PEB} = 130^\circ\text{C}$, $t_{PEB} = 60$ s and $t_{DEV} = 90$ s were repeated six times to estimate the reproducibility of the experiment.

PROLITH/2 is capable of using the rate expression shown in Eq. (14) to simulate profiles. The method of profile simulation using the generalized characteristic model is discussed elsewhere.⁹ SNR248 properties used in the simulations are summarized in Table 2 along with appropriate references.

4 Results

Figures 2(a), 2(b), and 2(c) show experimental measurements of τ_N , $\Delta\tau_{PEB}$, and $\Delta\tau_{DEV}$ as a function of incident

Table 1 Range of T_{PEB} , t_{PEB} , t_{DEV} investigated.

	Low	High
Postbake Temperature ($^\circ\text{C}$)	110	150
Postbake Time (s)	15	90
Develop Time (s)	30	120

Table 2 SNR248 simulation parameters.

Parameter	Value
k_{photo} (cm^2/mJ)	0.004
A (μm^{-1})	-0.71^7
B (μm^{-1})	1.10^7
Refractive Index	1.80
Resist Thickness (μm)	1.0

dose resulting from SNR248 processed at the centerpoint conditions ($T_{PEB} = 130^\circ\text{C}$, $t_{PEB} = 60$ s, $t_{DEV} = 90$ s). Data in Fig. 2(c) ($\Delta\tau_{DEV}$ versus dose) were regressed to extract αn and E_0 according to Eq. (13) to evaluate the develop rate expression [Eq. (14)]. Due to slight film loss during PEB, $\Delta\tau_{PEB}$ could not be measured precisely [see Fig. 2(b)]. Consequently, we were unable to regress α reliably from $\Delta\tau_{PEB}$ data. Figures 2(a), 2(b), and 2(c) show data from one run along with regressions for τ_N and $\Delta\tau_{DEV}$. Simulations with PROLITH/2 were done using αn and E_0 parameters regressed from $\Delta\tau_{DEV}$. The resulting simulated profiles were compared with experimental results. Figure 3 shows an example.

Table 3 summarizes regressed αn and E_0 parameters extracted from characteristic curves generated over the design of experiment conditions. Table 4 compares experimental and PROLITH/2 simulated linewidth measurements using αn and E_0 parameters extracted with the generalized characteristic model.

5 Discussion

5.1 Generalized Characteristic Model Form

The form of Eqs. (13) and (14) deserves further discussion. We note that at low ($E \approx E_0$) and high ($E \rightarrow \infty$) doses, both τ_N and r_{DEV} yield physically reasonable results. At $E = E_0$, $\tau_N = 0$ and $r_{DEV} = [D(1 - \Delta\tau_{PEB, E_0})]/t_{DEV}$. The latter is the average develop rate through the bulk of the resist remaining after postexposure bake at E_0 . At $E \rightarrow \infty$, $\tau_N \rightarrow 1 - \Delta\tau_{PEB, E_0}$ and $r_{DEV} \rightarrow 0$ provided that $\alpha > 0$. By inspecting the definition of α , this implies that the resist contains a photoacid generator and that both k_{PEB} and t_{PEB} are greater than 0.

The role of α in the chemical amplification process can

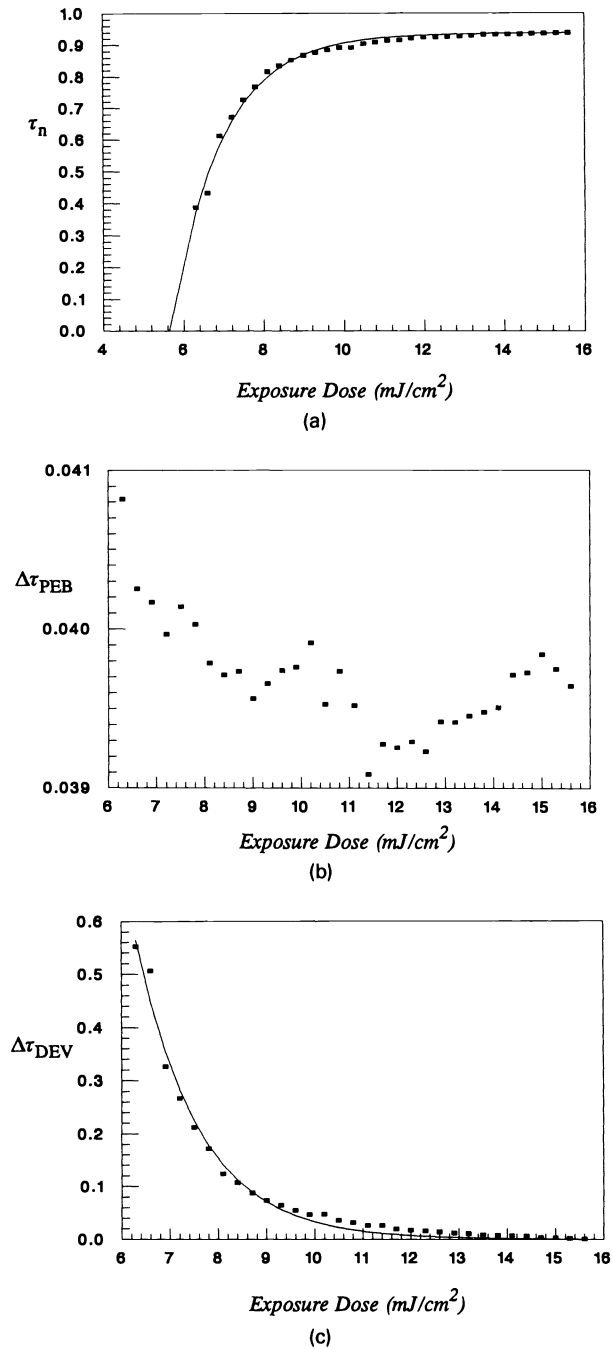


Fig. 2 (a) τ_n , (b) $\Delta\tau_{PEB}$, and (c) $\Delta\tau_{DEV}$ as a function of incident dose.

be discerned by deriving the characteristic curve for a conventional negative resist system. For this case, we assume that the soluble species is made insoluble by the photolysis alone:

$$\frac{d[S]}{dE} = -k_{photo}[S] \quad (15)$$

Substituting into Eqs. (5) and (1) and substituting in terms of E_0 for the case in which $\Delta\tau_{PEB} = 0$, we obtain:

$$\Delta\tau_N = 1 - \exp[-nk_{photo}(E - E_0)] \quad (16)$$

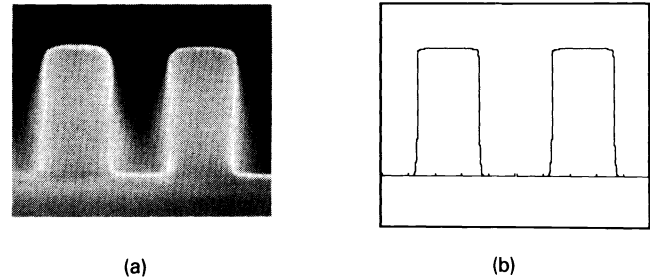


Fig. 3 (a) Experimental and (b) simulated SNR248 linewidths (nominal 0.5- μm lines and spaces).

Table 3 Characteristic model regression results.

Run	T_{PEB} (C)	t_{PEB} (s)	t_{DEV} (s)	$\alpha n \pm \text{Std Error}$	$E_0 \pm \text{Std Error}$ (mJ/cm ²)
Reproducibility Runs					
3a	130	60	90	183.7 \pm 5.4	5.39 \pm 0.06
3b	130	60	90	198.1 \pm 6.6	5.64 \pm 0.04
3c	130	60	90	171.5 \pm 8.1	5.24 \pm 0.10
3d	130	60	90	186.7 \pm 6.6	5.48 \pm 0.07
3e	130	60	90	197.3 \pm 8.2	5.53 \pm 0.07
3f	130	60	90	172.8 \pm 5.4	5.28 \pm 0.06
Constant t_{PEB}, t_{DEV}					
1	110	60	90	65.0 \pm 2.8	12.03 \pm 0.18
2	120	60	90	110.3 \pm 3.4	7.63 \pm 0.08
3*	130	60	90	185.0 \pm 6.7	5.43 \pm 0.07
4	140	60	90	197.0 \pm 9.4	4.08 \pm 0.09
5	150	60	90	216.2 \pm 6.2	2.56 \pm 0.04
Constant T_{PEB}, t_{DEV}					
7	130	15	90	107.7 \pm 2.4	7.71 \pm 0.06
8	130	38	90	134.8 \pm 5.2	5.69 \pm 0.09
3*	130	60	90	185.0 \pm 6.7	5.43 \pm 0.07
10	130	83	90	182.1 \pm 6.9	5.04 \pm 0.06
11	130	105	90	178.3 \pm 7.8	4.60 \pm 0.08
Constant T_{PEB}, t_{DEV}					
12	130	60	30	123.4 \pm 2.3	2.98 \pm 0.02
13	130	60	60	171.5 \pm 4.2	4.76 \pm 0.04
3*	130	60	90	185.0 \pm 6.7	5.43 \pm 0.07
14	130	60	120	126.7 \pm 5.1	5.20 \pm 0.12
15	130	60	150	138.4 \pm 6.2	5.90 \pm 0.12

*Average of six runs

Comparison with the expression for chemical amplification is made by investigating the case in which $\Delta\tau_{PEB} \approx 0$ and $\exp(-k_{photo}E) \approx 1 - k_{photo}E$. In such a case the characteristic curve for negative chemically amplified resists reduces to:

$$\tau_N = 1 - \exp[-\alpha nk_{photo}(E - E_0)] \quad (17)$$

Consequently, we observe that α amplifies the chemical reaction through a postexposure bake. Chemical amplification occurs for processing conditions in which α is greater than 1.

5.2 Comparison with Other Models

Several noteworthy comparisons can be made between the Generalized Characteristic Model and other lithography models. First, k_{photo} is identical to the C parameter in the model for conventional resists proposed by Dill et al.¹² The rate model ($r_{DEV} \propto [S]^n$), used to derive the generalized

Table 4 Measured and simulated linewidths.

Run	Dose (mJ/cm ²)	Linewidth (μm)		% Difference
		Measured [†]	Simulated	
1	67.8	0.459	0.39	15
2	33.0	0.43	0.405	6
3	30.9	0.512	0.493	4
4	30.9	0.623 [‡]	Scum	-
5	12.3	Scum	Scum	-
7	33.0	0.443	0.407	8
8	33.0	0.518	0.477	8
10	30.9	0.59	0.507	14
12	30.9	0.577	0.551	5
13	30.9	0.534	0.525	2
14	33.0	0.536	0.487	11
15	33.0	0.537	0.478	11

[†]Linewidths were measured by top down SEM.

[‡]Linewidths greater than 0.6μm were typically scummed when viewed from cross section

characteristic model, has been previously applied to conventional positive photoresists. Mack derived a general rate expression¹⁰:

$$r_{\text{DEV}} = r_{\text{MAX}} \frac{(a+1)(1-m)^n}{a+(1-m)^n} + r_{\text{min}} \quad (18)$$

For many photoresist systems, $a \gg 1$, which simplifies Eq. 18 to:

$$r_{\text{DEV}} = r_{\text{max}}(1-m)^n + r_{\text{min}} \quad (19)$$

Since $(1-m)$ is the concentration of the base soluble carboxylic acid, we recognize that the develop model proposed here is consistent with Mack's, provided r_{min} is negligible. Development rate expressions proportional to a power of a soluble species were also proposed by Daniels and Trefonas¹¹ and Hirai et al.¹³ though the underlying assumptions were different. Ferguson et al.⁷ used a similar functional form for r_{DEV} to model negative DUV resists:

$$r_{\text{DEV}} = R_0 \left[1 - \frac{CE_{(cs)}}{C_0} \right]^a, \quad (20)$$

where R_0 , C_0 , and a are regressed from develop rate data and C_{as} is obtained from acid-catalyzed crosslinking kinetics. If $[1 - CE_{(cs)}/C_0]$ is an effective soluble species concentration, then this model is equivalent to the one used in this paper.

5.3 Experimental and Predicted αn and E_0 Dependencies

It is interesting to compare predicted and measured effects on both E_0 and αn . To investigate E_0 , we solve Eq. (12) for E_0 :

$$E_0 = \frac{-\ln \left\{ 1 + \frac{\ln[D/(k_{\text{DEV}}t_{\text{DEV}}[S_0]^n)]}{\alpha n \exp(-k_{\text{photo}}E_{\text{inhib}})} \right\}}{k_{\text{photo}}} + E_{\text{inhib}}, \quad (21)$$

where $\Delta\tau_{\text{PEB}}$ was neglected for simplicity. We can expand Eq. (21) in a Taylor series:

$$E_0 = E_{\text{inhib}} + \frac{1}{k_{\text{photo}}} \left[\frac{\ln(k_{\text{DEV}}t_{\text{DEV}}[S_0]^n/D)}{\alpha n \exp(-k_{\text{photo}}E_{\text{inhib}})} \right] - \frac{1}{2k_{\text{photo}}} \left[\frac{\ln(k_{\text{DEV}}t_{\text{DEV}}[S_0]^n/D)}{\alpha n \exp(-k_{\text{photo}}E_{\text{inhib}})} \right]^2 + \dots \quad (22)$$

Therefore, as a first approximation:

1. E_0 is linearly dependent on logarithm of develop time and initial resist thickness.
2. E_0 is linear with the inverse of αn . Since α contains a rate constant, we expect E_0 to have an Arrhenius temperature dependence; that is, the logarithm of E_0 should be linearly dependent on $1/T_{\text{PEB}}$. Also since α is linear in postexposure bake time, E_0 should be inversely proportional to $1/t_{\text{PEB}}$.

Note that these are the same conclusions that can be obtained by approximating $1 - \exp[-k_{\text{photo}}(E - E_{\text{inhib}})] \approx k_{\text{photo}}(E - E_{\text{inhib}})$ in Eq. (12) and then solving for E_0 . Figures 4(a), 4(b), and 4(c) compare predicted dependencies of E_0 against experimental data.

From the definition of αn , we expect αn to be linearly dependent on t_{PEB} , independent of t_{DEV} , and exponentially dependent on $1/T_{\text{PEB}}$. Figures 5(a), 5(b), and 5(c) show experimental results over the conditions employed. Note that αn saturates as a function of higher postexposure bake temperatures (low $1/T_{\text{PEB}}$) and longer times. Furthermore, αn varied somewhat randomly with t_{DEV} .

Comparing Figs. 4 and 5, it is apparent that the predicted trends for E_0 agreed better with experiment than those for αn . One explanation is that n is processing dependent whereas the analysis above assumes a constant value. However, note that E_0 should be similarly affected. Two explanations are consistent with the observation that E_0 follows predicted trends while αn does not. First we note that since E_0 basically is extrapolated from $\Delta\tau_{\text{DEV}}$, it is most affected from data at relatively low $[H^+]$. In comparison, αn is calculated from $\Delta\tau_{\text{DEV}}$ data ranging from low to high proton concentrations. Therefore, we postulate that an effective acid-quenching mechanism at larger proton concentrations limits αn under conditions for which the GCM model would predict higher proton concentrations (higher postexposure bake temperature and time). Note that the existence of an "acid loss" reaction has indeed been proposed by Ferguson et al.⁷

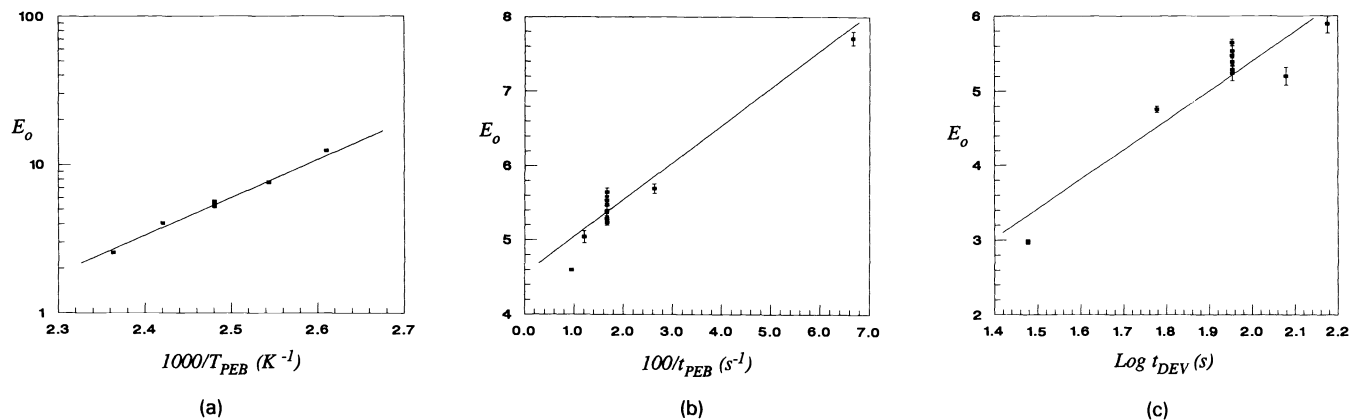


Fig. 4 Experimental E_0 dependence on (a) T_{PEB} , (b) t_{PEB} , and (c) t_{DEV} (error bars show \pm one standard error).

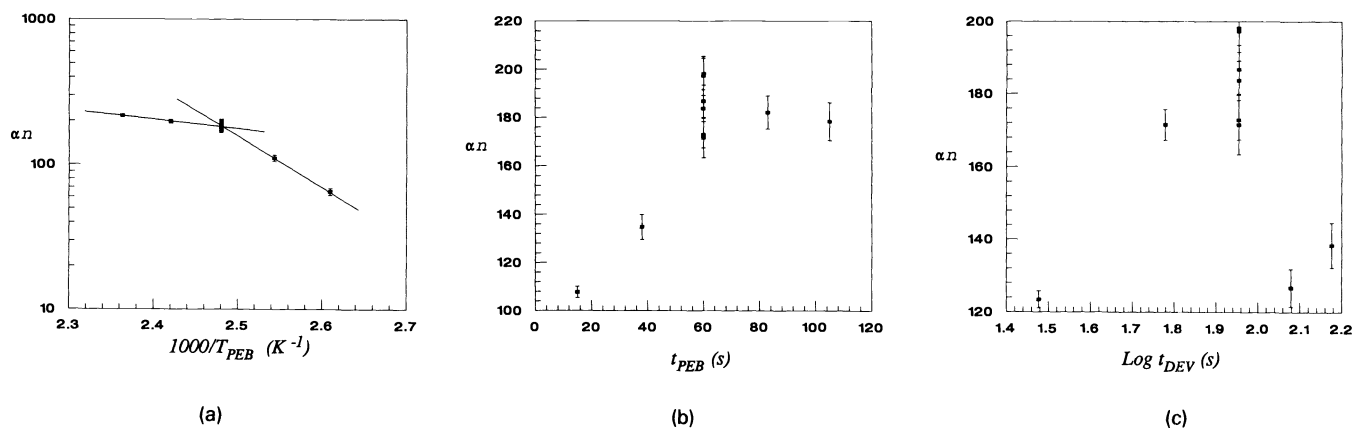


Fig. 5 Experimental αn dependence on (a) T_{PEB} , (b) t_{PEB} , and (c) t_{DEV} (error bars show \pm one standard error).

Alternatively, the insolubilization reaction could be limited by proton diffusion at higher postexposure bake temperatures and times. Consequently, E_0 follows the predicted T_{PEB} , t_{PEB} , and t_{DEV} trends at low $[H^+]$, but quenching or diffusion limits the insolubilizing reaction thus limiting αn under conditions that should yield higher proton concentrations. In fact, close inspection of the Arrhenius plot [Fig. 5(a)] shows evidence for two activation energies above (2.6 kcal/mol) and below 130°C (16 kcal/mol), while αn is linear with t_{PEB} at low times and levels off at longer times. The average activation energy calculated from αn data below 130°C (16 kcal/mol) compares to 12 kcal/mol regressed from E_0 data from 110 to 150°C . It is interesting that the activation energy for αn at the lower extent of the reactions (16 kcal/mol) and E_0 computed throughout the entire temperature range compare favorably with the measured sensitivity dose activation energy of 13.4 kcal/mol reported by Seligson, Das, and Gaw³ for a similar negative chemically amplified resist.

Finally, it is worthwhile to recognize the effect that E_{inhib} has on both the characteristic curve and bulk develop rates. Note that E_{inhib} does not appear as an independent parameter

but is lumped into E_0 . Physically, this means that impurities requiring neutralization that are uniformly distributed in the resist will decrease the sensitivity of the resist but not the exposure dependence (i.e., contrast). This is not true for positive chemically amplified resist systems in which impurities are expected to decrease the sensitivity and lower the bulk contrast.⁹

6 Conclusions

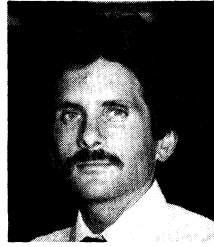
The application of the Generalized Characteristic Model for lithography toward modeling negative chemically amplified resists is demonstrated. In this technique, relevant lumped parameters are extracted from experimental characteristic curves. These parameters are then used to evaluate effective develop rates in lithographic simulation. Simulated linewidths agreed within 15% of measured values over the entire processing window without using adjustable parameters. The dependence of the lumped parameters on process conditions was explored. While E_0 followed the predicted trends of T_{PEB} , t_{PEB} , and t_{DEV} , αn did not. A possible explanation is that quenching of the $[H^+]$ catalyst at higher conversions causes this discrepancy.

Acknowledgments

The authors wish to acknowledge the following individuals at SEMATECH for their contributions: Setyandra Sethi for the experimental work, Orlando Castanon for all SEM work, and William Connor for statistical consultation. Discussions with Charles Szmanda and Jim Thackery (Shibley Co.) concerning SNR248 chemistry were extremely valuable toward the development of the Generalized Characteristic Model approach. We also acknowledge useful conversations with Richard Ferguson, Andrew Neureuther, and William Oldham from the University of California, Berkeley, and Eytan Barouch of Princeton University.

References

1. J. W. Thackeray, G. W. Orsula, D. Canistro, E. K. Pavelchek, L. E. Bogan, A. K. Berry, and K. A. Graziano, "DUV ANR photoresists for 248nm excimer laser photolithography," *Proc. SPIE* **1086**, 34 (1989).
2. H. Ito, L. A. Pederson, K. N. Chiong, S. Sonchik, and C. Tsai, "Sensitive electron beam resist systems based on acid-catalyzed deprotection," *Proc. SPIE* **1086**, 11 (1990).
3. D. Seligson, S. Das, H. Gaw, and P. Pianetta, "Process control with chemical amplification resists using deep ultraviolet and x-ray radiation," *J. Vac. Sci. Technol.* **B6**, 2303 (1988).
4. S. Das and D. Seligson, "Characterization and process control of thermally activated resists," *Proc. 1988 International Photopolymers Conf.* Ellenville, New York.
5. S. Das, J. Thackeray, M. Endo, J. Langston, and H. Gaw, "A systematic investigation of the photoresponse and dissolution characteristics of an acid hardening resist," *Proc. SPIE* **1262**, 60 (1990).
6. H. Fukuda and S. Okazaki, "Kinetic model and simulation for chemical amplification resists," *J. Electrochem. Soc.* **137**, 675-679 (1990).
7. R. A. Ferguson, J. M. Hutchinson, C. A. Spence, and A. R. Neureuther, "Modeling and simulation of a deep-ultraviolet acid hardening resist," *J. Vac. Sci. Technol.* **B8**, 1423 (1990).
8. A. S. Chiu, R. A. Ferguson, T. Doi, A. Wong, and A. R. Neureuther, "Resist parameter extraction (PARMEX) with graphical user interface in X," *Proc. SPIE* **1466**, 641 (1991).
9. D. H. Ziger and C. A. Mack, "A generalized approach towards modeling resist chemistry," *AIChE J.* **37**, 1863 (1991).
10. C. A. Mack, "PROLITH: a comprehensive optical lithography model," *Proc. SPIE* **538**, 207 (1985).
11. P. Trefonas and B. K. Daniels, "New principle for image enhancement in single layer positive photoresists," *Proc. SPIE* **771**, 194 (1987).
12. F. H. Dill, W. P. Hornberger, P. S. Hauge, and J. M. Shaw, "Characterization of positive photoresist," *IEEE Trans. Electron Dev.* **ED-22**, 445 (1975).
13. Y. Hirai, M. Sasago, M. Endo, K. Tsuji, and Y. Mano, "Process modeling for photoresist development and design of DLR/sd process," *IEEE Trans. Computer-Aided Des.* **CAD-6**, 403 (1987).



David H. Ziger received a BS in chemical engineering from the University of Wisconsin in 1978 followed by MS (1980) and Ph.D. degrees (1983), also in chemical engineering, from the University of Illinois. Ziger joined AT&T Bell Laboratories Engineering Research Center in Princeton, New Jersey, in 1983 where he worked in advanced lithography development programs. From 1989-91 he managed the Advanced Resist Program at SEMATECH as an AT&T Bell Laboratories assignee. Currently, Ziger is a member of the AT&T Bell Laboratories Advanced Lithography Group in Allentown, Pennsylvania. He has patents and publications in areas ranging from high-pressure thermodynamics to statistical control techniques to advanced lithography methods.



Chris A. Mack received BS degrees in physics, chemistry, electrical engineering, and chemical engineering from Rose-Hulman Institute of Technology in 1982 and an MS degree in electrical engineering from the University of Maryland in 1989. He joined the Microelectronics Research Laboratory of the Department of Defense in 1983 and began work in optical lithography research. He has authored numerous papers in the area of optical lithography, regularly teaches courses on this topic, and has developed the lithography simulation programs PROLITH and PROLITH/2. He is currently on assignment at SEMATECH.



Romelia Distasio graduated from San Jose State University with a BS in social services in 1978. Distasio was involved in various phases of lithographic processing at Signetics (1979-82), Trilogy (1982-84) and Intel (1985-88). In 1988, she joined the Resist Processing Group at SEMATECH in Austin, Texas, where she implements advanced *i*-line and DUV resist processes.